THE JOURNAL OF BIOLOGICAL CHEMISTRY VOL. 284, NO. 32, pp. 21659–21669, August 7, 2009

Sorting Nexin 33 Induces Mammalian Cell Micronucleated Phenotype and Actin Polymerization by Interacting with Wiskott-Aldrich Syndrome Protein*[S]

Received for publication, April 11, 2009, and in revised form, May 20, 2009 Published, JBC Papers in Press, June 1, 2009, DOI 10.1074/jbc.M109.007278

Juan Zhang[‡§1], **Xiaofei Zhang**[§1], **Yunqian Guo**[‡§1], **Liangliang Xu**[‡§1], **and Duanqing Pei**[§2]

From the [‡]*Laboratory of Stem Cell Biology, Department of Biological Sciences and Biotechnology, Institute of Biomedicine, School of Medicine, Tsinghua University, Beijing 100084, China and the* [§]*Stem Cell and Cancer Biology Group, Key Laboratory of Regenerative Biology, South China Institute for Stem Cell Biology and Regenerative Medicine, Guangzhou Institutes of Biomedicine and Health, Chinese Academy of Sciences, Guangzhou 510663, China*

Sorting nexin 33 (SNX33) is a novel member of the sorting nexin superfamily with three predicted structural domains, SH3-PX-BAR. Very little is known about the cellular function of SNX33. In an effort to analyze its structure/function relationship, we attempted but failed to generate stable cell lines for short hairpin RNA or overexpression SNX33. Transient knockdown of SNX33 induces both HeLa and MCF7 cells to grow multiple long processes, delay the G_1/M transition, and become more apoptotic, implying that SNX33 may control cell cycle process through influence the cytoskeleton. *In vitro* cell lineage analysis revealed that cells transfected with SNX33 failed to divide and became micronucleated, suggesting a specific defect in cytokinesis. Further analysis revealed that SNX33 induced the accumulation of actin at the perinuclear space, which might have disabled the cytokinetic machinery. However, SNX33 appears to mediate actin polymerization indirectly, as they do not interact with each other. SNX33 interacts with itself and SNX9. Interestingly, it also interacts with VCA domain of Wiskott-Aldrich syndrome protein (WASp), a protein known to be involved in actin polymerization. Indeed, cells overexpressing WASp failed to divide and form stable colonies as SNX33, consistent with the notion that SNX33 may interfere with cytokinesis. On the other hand, knockdown of WASp alleviates the phenotype induced by SNX33. Taken together, our results suggest that SNX33 plays a role in maintaining cell shape and cell cycle progression through its interaction with WASp.

Among SNX (sorting nexin) family, SNX1 was first identified by yeast two-hybrid selection for epidermal growth factor receptor binding partners (1), which also include SNX2, SNX3, and SNX4 (2). Interestingly, SNX1, SNX2 and SNX4 appear to interact with each other (3–5). Subsequently, more SNXs were discovered based on sequence homology, including SNX5 as a putative Fanconi anemia complementation group A-binding protein (6), SNX6 (7), and SNX9 (8, 9). SNX10 was discovered by its ability to induce vacuoles in mammalian cells (10). To date, 33 SNXs have been reported in mammalian genomes, and they can be classified into three major groups; (i) SNX^{PX} (SNX3, -10, -12, -22, and -24); (ii) $SNX^{PX\text{-}BAR}$ (SNX1, -2, -4–9, -18, -30, -32, and -33); (iii) $SNX^{PX\text{-}other}$(SNX11, -13–17, -19–21, -25, -27, -29, and -31) (11). The physiological function of these SNXs remains poorly understood.

SNX33 is a novel SNX with three conserved domains: SH3, PX, and BAR. Recent studies suggest that SNX33 may function to regulate endocytic process and α-secretase cleavage process of the amyloid precursor protein (12) and the formation of PrP (13). These functions are similar to those reported for SNX9, a close relative of SNX33. SNX9 was identified as a binding partner for MDC9 and MDC15 (8). It appears that SNX9 functions through ACK2 to regulate epidermal growth factor receptor degradation with necessary dimerization of itself (9, 14), Wiskott-Aldrich syndrome protein (WASp) in T cells (15), and multiple phosphoinositides to direct membrane remodeling (16). Furthermore, SNX9, when overexpressed in 3T3L1 adipocytes, can co-immunoprecipitate with insulin receptor and decrease insulin receptor binding (17). These findings suggest that SNX9 regulates endocytosis, remodels membrane structure, and serves as a bridging mediator between membrane and cytoskeleton.

WASp, the protein encoded by the gene for the Wiskott-Aldrich syndrome protein, contains WH1, BR, the GTPase binding, proline-rich, and VCA domains and plays an essential role in actin polymerization (18). The VCA domain interacts with ARP2/3, and phosphorylation of the VCA domain enhances this interaction, which leads to actin polymerization (19–21). Activation of WASp triggers abnormal mitosis and cytokinesis with multi-nucleate phenotype (22).

In this paper we report the cloning and characterization of a novel sorting nexin, SNX33. SNX33 was cloned from HEK293T cells, and it showed a very extensive expression profile according to the cells lines we tested. We found that knockdown of SNX33 caused HeLa or MCF7 cell morphology change, which may influence the cell cycle and apoptosis ratios of these two

* This work was supported by National Natural Science Foundation of China Grants 30630039, 30725012, 30700410, 30871404, and 90813033; by Knowledge Innovation Project of The Chinese Academy of Sciences Grants KSCX2-YW-R-48 and KSCX1-YW-02-1; by Bureau of Science and Technology of Guangzhou Municipality, China, Grant 2008A1-E4011; and by 973 Program of China Grants 2006CB701504, 2006CB943600, 2007CB948002, 2007CB947804, 2007CB947900, 2009CB941102 and 2009CB940902.

[S] The on-line version of this article (available at http://www.jbc.org) contains supplemental data.

[1] These authors contributed equally to this work.

[2] To whom correspondence should be addressed. Tel.: 011-86-20-3229-0706; E-mail: pei_duanqing@gibh.ac.cn.

TABLE 1
Primers for cloning

Gene	Forward sequence (5′–3′)	Reverse sequence (5′–3′)
SNX1-F	accatggcgtcgggtggtggtggctgtag	ggagatggcctttgcctcaggaaggaag
SNX2-F	accatggcggccgagagggaacctcctcc	ggcaatggctttggcttcaggtaggaatgc
SNX3-F	accatggcggagaccgtggctgacacc	ggcatgtcttattttagatggagtatagctttt
SNX9-F/Myc	accatggccaccaaggctcgggttatgtat	tcactggaaagcggctgagggcctgcct
SNX33-(GFP)F	accatggcactgaaaggccgagccctctatg	gaggttgtcatacatgcgcagggtc
(Myc)-GFP-SNX33	accatggcactgaaaggccgagccctctatg	tcagaggttgtcatacatgcgcagggtc
GFP-D1	accatggcactgaaaggccgagccctctatg	tcaggtgctgatgccagaacggacgatc
GFP-D2	accatggcactgaaaggccgagccctctatg	tcagaggttgtcatacatgcgcagggtc
GFP-D3	accatggcactgaaaggccgagccctctatg	ggcacccaccatctcatccttctcc
GFP-D4	accatggccaagatcgctgagacatactcca	tcaggcacccaccatctcatccttctcc
GFP-D5	accatggccaagatcgctgagacatactcca	tcagaggttgtcatacatgcgcagggtc
GFP-D6	accatggatgacaagcagtggaagatgggca	tcagaggttgtcatacatgcgcagggtc
SNX33-D2F	accatggcactgaaaggccgagccctctatg	aatggagtatgtctcagcgatc
SNX33-D3F	accatggcactgaaaggccgagccctctatg	ggcacccaccatctcatccttctcc
SNX33-D5F	accatggccaagatcgctgagacatactcca	gaggttgtcatacatgcgcagggtc
SNX33-D6F	accatggatgacaagcagtggaagatgggca	gaggttgtcatacatgcgcagggtc
(Myc)-GFP-SNX33-D7	accatggactactccagcagccctgcaggct	tcagaggttgtcatacatgcgcagggtc
F/GFP-WASP	accatgagtgggggcccaatgggaggaagg	tcagtcatcccattcatcatcttcatc
WASp-D1	accatgagtgggggcccaatgggaggaagg	tcaagatggcggtgggggcggcggaag
WASp-D2	accatgcgaggagggaaccagctcccccgg	tcagtcatcccattcatcatcttcatc
WASp-D3	accatgagtgggggcccaatgggaggaagg	tcacttcttcttccctgagcgtttctta
WASp-D4	accatgagtgggggcccaatgggaggaagg	tcaaagctgtgagtacagctcctgttcc
WASp-D5	accatggtctactccaccccccacccccttct	tcagtcatcccattcatcatcttcatc
WASp-D6	accatggctctggtgcctgccgggggcctgg	tcagtcatcccattcatcatcttcatc
SNX9	accatggccaccaaggctcgggttatgtat	tcactggaaagcggctgagggcctgcct
SNX9ΔSH3	accatgagtgatggaaaagatcaattttcttgtg	tcactggaaagcggctgagggcctgcct

cell lines. We proved that SNX33 was very important for cell survival because overexpression of SNX33 in HeLa cells gives rise to cell death with micronuclei phenomena. SNX33 does behave like the other members in the SNX family, in that SNX33 can form homodimers by itself and form heterodimers with SNX9, which is another member in the same subfamily. We further demonstrated that SNX33 can bind to WASp, enhance actin polymerization, and induce abnormal cytokinesis process. As far as we know this is the first report that associates SNX33 with WASp and actin polymerization.

EXPERIMENTAL PROCEDURES

Reverse Transcriptase-PCR Analysis—Total RNA (2 μg) was reverse-transcribed in a final volume of 20 μl. PCR was performed for 28 cycles (SNX33) or 18 cycles (actin), respectively. The primers used were: human SNX33 reverse transcriptase (RT) forward, 5′-ctctctaccagggcctgctctccaacttc-3′, and reverse, 5′-gaggttgtcatacatgcgcagggtc-3′; human actin RT forward, 5′-aagctgtgctacgtcgccctggacttcgag-3′, and reverse, 5′-agaagcatttgcggtggacgatggaggggc-3′.

Expression, Purification of Human SNX33, and Preparation of Anti-SNX33 Antibodies—Full-length human SNX33 cDNA was inserted into the SmaI site in the modified vector PET-32a. Human SNX33 protein was expressed in BL21-DE3 as described (23) and stored at −80 °C. Purity was subjected to SDS/PAGE and Coomassie blue staining. Rabbit polyclonal antibodies against human SNX33 were prepared and purified as described (23).

Plasmid Construction—Human SNX33 and WASp open reading frames were amplified by PCR using high fidelity polymerase *KOD taq* (TOYOBO) from mRNA isolated from HEK293T cells and then inserted individually into the EcoRV site of the modified pCR3.1II with GFP and Myc tags at the N terminus or FLAG tag at the C terminus (24). cDNAs for SNX1, SNX2, SNX3, SNX9 were purchased from ATCC (Manassas, VA) and subcloned into the modified pCR3.1 with a FLAG or Myc tag at the C terminus. F-WASp was subcloned into the PmeI site of the modified pPyCAGIP vector (a kind gift from Dr. Ian Chamber, University of Edinburgh) with a FLAG tag at the N terminus. Deletions of human WASp (WASp-D1, WASp-D2, WASp-D3, WASp-D4, WASp-D5, WASp-D6) were subcloned by inserting PCR products into the EcoRV site of the modified pCR3.1II with GFP and Myc tags at the N terminus (25). Deletions of human SNX33 (D2F, D3F, D5F, D6F) were generated by inserting PCR products into a modified pCR3.1 vector with a FLAG tag at the C terminus. Deletions of human SNX33 with GFP fusion (GFP-D1, GFP-D2, GFP-D3, GFP-D4, GFP-D5, GFP-D6, GFP-D7), SNX9, and its deletion SNX9ΔSH3 were cloned into a modified pCR3.1II vector with GFP and Myc tags at the N terminus. The control, shRNA1, and shRNA2 plasmids were kind gifts from Dr. Stefan F. Lichtenthaler (Ludwig Maximilians University). All constructions were confirmed by DNA sequencing. Primers for cloning are shown in Table 1.

Cell Culture, Transfection, and FACS[3]—Cells were cultured in Dulbecco's modified Eagle's medium (for HEK293T cells, Invitrogen) or RPMI medium 1640 (for A549, pro5, PC3, SPC-A1, NCI-H460, HT1080, Hlamp, LN4, GLC82, L-78, MCF7, and HeLa cells, Sigma) supplemented with 10% fetal bovine serum (Hyclone) and 100 μg/ml antibiotics (penicillin and streptomycin, Invitrogen). HeLa cells, MCF7 cells, and HEK293T cells were transfected by Lipofectamine 2000 (Invitrogen). The transfection of short interfering RNA (siRNA) was performed using Lipofectamine 2000 (Invitrogen). Sense siRNA sequences targeting WASp or control sequences were: siWASp-1, TGAGATGCTTGGACGAAAA; siWASp-2, GAATCAGAGGCAAAGTGGA; siControl, CGGCCAGATCTCAATATCAT (26, 27). For cell cycle analysis, cells were stained with BD Cycletest™ Plus DNA Reagent kit and analyzed by FACScalibur (BD Biosciences). For apopto-

[3] The abbreviations used are: FACS, fluorescence-activated cell sorter; SNX, sorting nexin; siRNA, small interfering RNA; TRITC, tetramethylrhodamine isothiocyanate; GFP, green fluorescent protein; shRNA, short hairpin RNA.

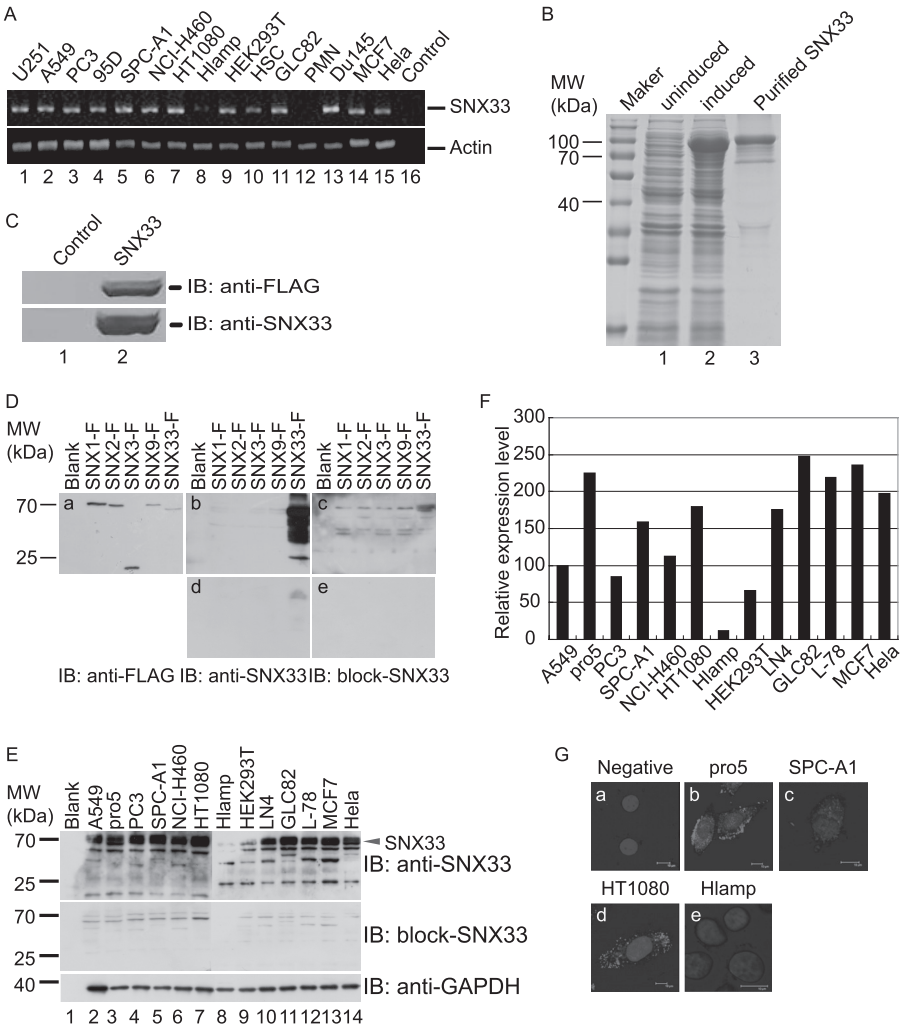

FIGURE 1. **Expression of SNX33 RNA and protein in various human cells.** *A*, RNA expression profile of SNX33 in 15 cell lines. Semiquantitative analysis of SNX33 expression was performed as described under "Experimental Procedures" with actin as the internal control. Note that PMN is negative, and Hlamp is low in SNX33 expression. *B*, prokaryotic expression of human SNX33. BL21-DE3 cells harboring His-SNX33 expression vector was induced to express the recombinant protein (*lane 3*) by using 1 mM isopropyl 1-thio-β-D-galactopyranoside. Recombinant SNX33 was purified by using Ni^{+} affinity chromatography and then analyzed by SDS-PAGE and stained with R250. *C*, generation and characterization of anti-human SNX33 antibodies. FLAG-tagged SNX33 expression plasmid and the control vector were transfected into HEK293T cells. Cell lysates were analyzed on a SDS/PAGE gel by using anti-FLAG antibodies and anti-SNX33 antibodies as first antibodies (1:5000) and then developed with ECL as described under "Experimental Procedures." *IB*, immunoblot. *D*, the anti-SNX33 antibody is mono-specific. Cell lysates of HEK293T cells transfected with control vector, SNX1-F, SNX2-F, SNX3-F, SNX9-F, or SNX33-F were fractionated on 12% SDS-PAGE and then electroblotted to polyvinylidene difluoride membrane. The proteins were detected by using anti-FLAG antibodies (*a*), anti-SNX33 antibodies (*b* and *d*), or anti-SNX33 antibodies pre-absorbed with SNX33 soluble proteins (*c* and *e*) as first antibodies, then detected with goat anti-mouse or goat anti-rabbit antibodies as secondary antibodies conjugated with horseradish peroxidase, and then developed with ECL. *E*, protein expression profile of human SNX33 in 13 cell lines. Cell lysates of 13 different cell lines quantified with DCA protein quantify kits were run on 12% SDS-PAGE and then electroblotted to polyvinylidene difluoride membranes. The proteins were detected by using anti-SNX33 antibodies, anti-SNX33 antibodies pre-absorbed with SNX33-soluble proteins, or anti-glyceraldehyde-3-phosphate dehydrogenase (*GAPDH*) as first antibodies, then detected with goat anti-mouse or goat anti-rabbit antibodies as secondary antibodies conjugated with horseradish peroxidase, and then developed with ECL. Note the *triangle*, indicating SNX33 proteins. *F*, quantification of SNX33 expression in *E* with glyceraldehyde-3-phosphate dehydrogenase as the internal reference. *G*, localization of endogenous SNX33 by confocal microscopy. Pro5, SPC-A1, HT1080, and Hlamp fixed in coverslips were stained with anti-SNX33 antibodies or pre-immunized serum as first antibodies and detected by using TRITC-conjugated goat anti-rabbit antibodies and then captured by Leica confocal systems. Note the negative staining of SNX33 in Hlamp.

sis assay, cells were treated by PE annexin V Apoptosis Detection Kit I (BD Biosciences) and analyzed by FACScalibur (BD Biosciences).

Stable Cell Line Selection and Live Cell Counting Assay—HeLa cells were seeded into 3.5-cm dishes and transfected with 2 μg of each expression plasmid by Lipofectamine 2000 (Invitrogen). 24 h after transfection cells were divided at 1:50 and seeded into new 10-cm dishes for selection. G418 (800 μg/ml, Merck) was added to the medium for selection. For cell counting, HeLa cells were seeded into 12-well plates and transfected with 1 μg of each expression plasmid by Lipofectamine 2000. 24 h post-transfection, cells were split at 1:100 and seeded to 96-well plates with 5 wells per transfection and then counted everyday. For counting micronuclei cells, HeLa cells were seeded in 12-well plates and transfected with 1 μg of each expression plasmid by Lipofectamine 2000. 24 h post-transfection, cells were fixed with 4% paraformaldehyde in PBS, stained for nuclei with 4′,6-diamidino-2-phenylindole (1:5000, Sigma), captured by Olympus digital cameral and counted.

Microscopy and Cell Staining—The morphologies of cells were photographed by Olympus digital cameral. For immuno-staining, cells grown on coverslips were fixed with 4% paraformaldehyde in phosphate-buffered saline, washed, blocked in 10% normal goat serum, then stained with first antibodies, including anti-SNX33 antibody (prepared in this study), anti-γ-tubulin antibody (Sigma), anti-FLAG antibody (Sigma), and anti-Myc antibody (Cell Signaling Technology), and then stained with goat anti-mouse IgG TRITC (Santa Cruz) or goat anti-rabbit IgG TRITC (Santa Cruz). F-actin filaments were detected by staining with rhodamine-phalloidin (Invitrogen). The images were acquired by a Leica confocal system.

Western Blot and Immunoprecipitation—For Western blotting analysis, HEK293T cells cultured in 24-well plates were transfected by Lipofectamine 2000 with expression plasmids (0.5 μg each). Cells were lysed in radioimmune precipitation assay buffer (50 mM Tris-HCl, pH 7.5, 150 mM NaCl, 0.25% sodium deoxycholate, 0.1% Nonidet P-40, 0.1% Triton X-100), electrophoresed with 10% SDS-PAGE, and blotted to polyvinylidene difluoride membranes (Millipore). The membranes were then

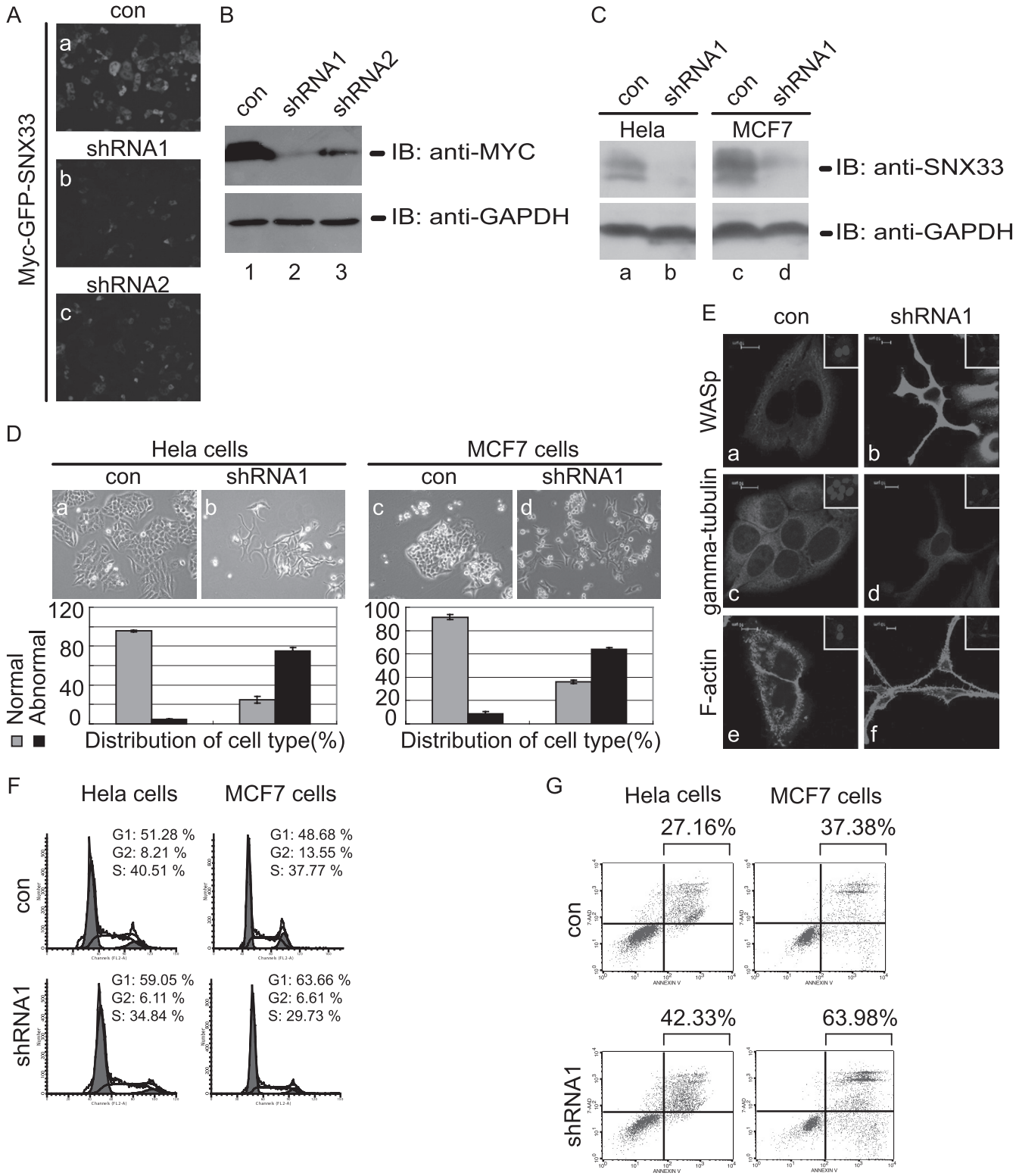

FIGURE 2. **shRNA knockdown of SNX33 results in dramatic cell shape change, cell cycle arrest, and apoptosis.** *A*, knockdown of exogenous SNX33 by shRNA1 and shRNA2. HEK293T cells transfected with control vector (*con*), shRNA1, or shRNA2 with GFP-tagged SNX33 for 24 h and then photographed for the GFP signal as described. Note the reduction of GFP signal in shRNA1- and shRNA2-treated cells. *B*, confirmation of SNX33 knockdown by Western blot (*IB*). *GAPDH*, glyceraldehyde-3-phosphate dehydrogenase. *C*, efficient knockdown of endogenous SNX33 in HeLa and MCF7 cells. The cell lysates were analyzed as described above. Note the effective reduction of SNX33 in shRNA1-treated cells (*panels b* and *d*). *D*, cell shape alteration as a result of SNX33 knockdown in HeLa or MCF7 cells. Cells transfected with control or shRNA1 were selected for hygromycin and photographed (*upper panels*). Cells with abnormal shape were counted and presented in the *lower panels*. Note that up to 80% of the cells observed are atypical in shape. *E*, immuno-staining of markers in SNX33 knockdown cells. Cells were grown in lips and fixed with 4% paraformaldehyde and then stained with the indicated antibodies. Note the cell shape changes, as indicated by signals from WASp and F-actin. *F*, cell cycle shift toward G_1 blockade in cells with SNX33 knockdown. Cells were stained by using BD Cycletest™ Plus DNA reagent kit and analyzed by FACScalibur (BD Biosciences). *G*, knockdown of SNX33 enhances apoptotic rate. Cells were treated by PE annexin V Apoptosis Detection Kit I (BD Biosciences) and then analyzed by FACScalibur (BD Biosciences).

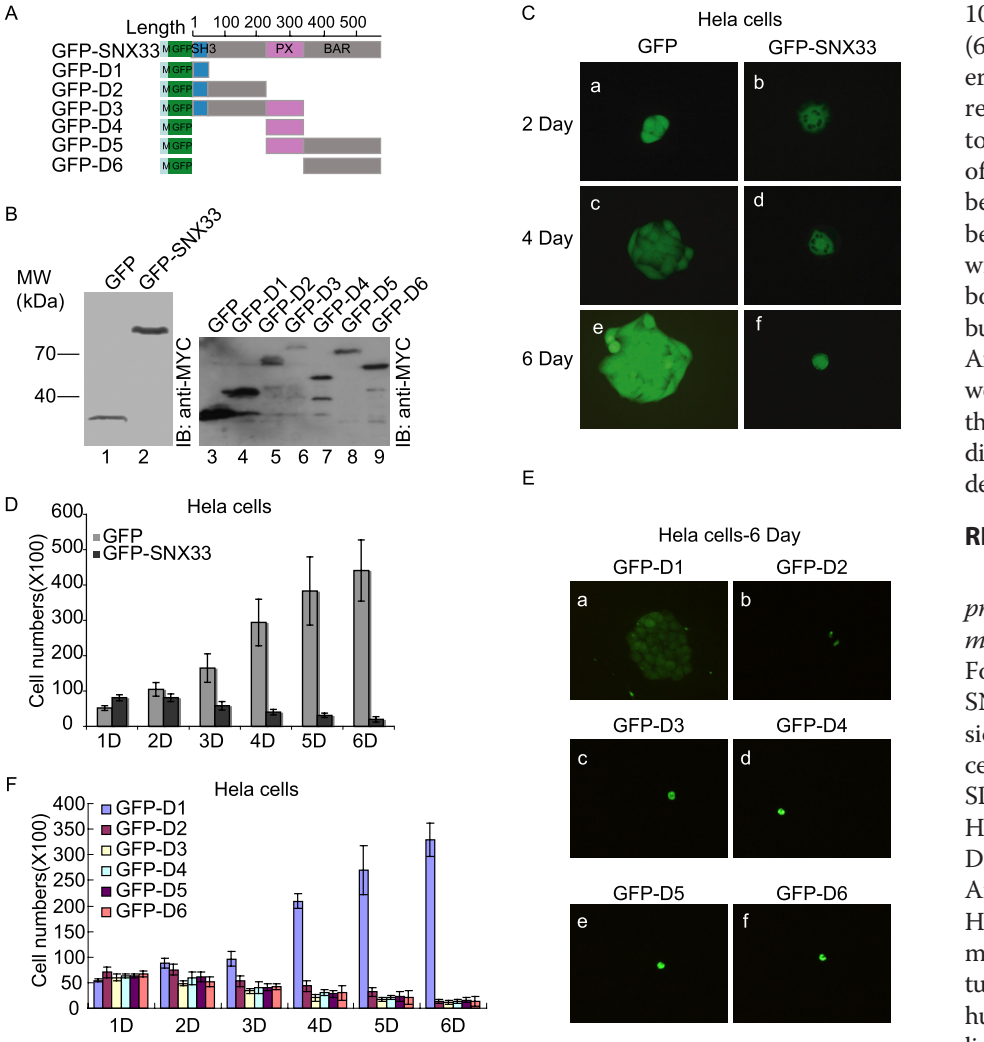

FIGURE 3. **Overexpression of SNX33 blocks cell division.** *A*, SNX33 deletion constructs. The domain structure of SNX33 fused to Myc-tagged GFP is shown on top with various deletions listed below. *SH3*, Src homology 3 domain; *PX*, phox homology domain; *BAR*, Bin/amphiphysin/Rvs domain. *B*, Western blot analysis of constructs listed in *A*. *C*, full-length SNX33 expression in HeLa cells blocks cell division. Clonal tracing demonstrates that cells transfected with GFP-tagged SNX33 (*b*, *d*, and *f*) failed to divide, whereas those with GFP were dividing normally (*a*, *c*, and *e*). *D*, growth curves of cells transfected with GFP or SNX33 in HeLa cells. HeLa cells transfected with GFP or GFP-tagged SNX33 (*GFP-SNX33*) were split into 96-well plate (5 wells each), and GFP-positive cells were counted daily. *E*, growth inhibitory effects of SNX33 deletions in HeLa cells. Cells transfected with the indicated deletions of SNX33 failed to grow, except the GFP-D1 deletion. *F*, growth curves of transfected cells in *E*. HeLa cells transfected with GFP-tagged SNX33 deletions (GFP-D1, GFP-D2, GFP-D3, GFP-D4, GFP-D5, GFP-D6) were cultured and counted daily to show the inhibitory effects of SNX33 domains.

blotted with 5% nonfat milk and incubated with anti-FLAG (1:5000, Sigma), anti-Myc (1:5000, Abcam), anti-SNX33 (1:5000, made by us), anti-glyceraldehyde-3-phosphate dehydrogenase (1:2000, Kang Chen), or anti-WASp (1:500, Abcam) antibodies followed by horseradish peroxidase-conjugated anti-mouse (1:5000, Sigma), anti-rabbit (1:5000, Sigma), or anti-goat (1:5000, Promega) secondary antibodies. The membranes were then washed extensively and developed with ECL (GE Healthcare).

For immunoprecipitation, the indicated plasmids were transfected into HEK293T cells by Lipofectamine 2000 (Invitrogen). 48 h after transfection cells were lysed in 400 μl of TNE buffer (50 mM Tris-HCl, pH 7.5, 150 mM NaCl, 0.5% Nonidet P-40, 1 mM EDTA, protease inhibitor mixture (Sigma)) on ice. Cell lysates were cleared by centrifugation at 13,000 $\times$ *g* for 10 min at 4 °C. Cleared cell lysates (60 μl) were saved for direct Western blotting analysis, and the remaining samples were transferred to a new tube containing 40 μl of anti-FLAG-conjugated-agarose beads (Sigma). The anti-FLAG beads were then washed 10 times with TNE buffer and then eluted by boiling for 5 min in 2% SDS loading buffer (with 5% β-mercaptoethanol). After centrifugation, supernatants were loaded on 12% SDS-PAGE and then blotted onto polyvinylidene difluoride membrane (Millipore) for detection.

RESULTS

Human SNX33 Is Widely Expressed in Various Cell Lines at Both mRNA Levels and Protein Levels—For functional study of human SNX33, we first tested the expression of human SNX33 in 15 human cell lines: U251, A549, PC3, 95D, SPCA1, NCIH460, HT1080, Hlamp, HEK293T, HSC, GLC82, PMN, Du145, MCF7, and HeLa cells. Among the above 15 cell lines, HEK293T, HSC, and PMN are normal cells or cell lines, the others are tumor cells. As shown in Fig. 1*A*, human SNX33 was detected in 13 cell lines except Hlamp and PMN; actin was taken as the internal control. These results indicate that human SNX33 expresses very widely.

To see if the human SNX33 protein is also expressed as widely as its mRNA, we generated polyclonal antibody against human SNX33 expressed in *Escherichia coli* (Fig. 1*B*, *lane 2*). Upon affinity purification against the recombinant protein coupled to agarose beads, the antibody could detect human SNX33 proteins with a FLAG tag much more efficiently than anti-FLAG antibody (Fig. 1*C*). To further test the specificity of anti-SNX33 antibody, we transfected FLAG-tagged SNX1 (SNX1-F), SNX2 (SNX2-F), SNX3 (SNX3-F), SNX9 (SNX9-F), or SNX33 (SNX33-F) and analyzed the expression of these proteins in lysates by Western blot with anti-FLAG or anti-SNX33 antibodies. As shown in Fig. 1*D*, SNX1, SNX2, SNX3, SNX9, and SNX33 expressed normally and specifically when using anti-FLAG antibody detection. When using anti-SNX33 antibody, only cell lysates expressing SNX33 could be detected. To further demonstrate the specificity of the SNX33 antibody, we preincubated the antibody with purified SNX33 protein before Western blotting. As shown in Fig. 1*D*, preabsorption of the antibody with the

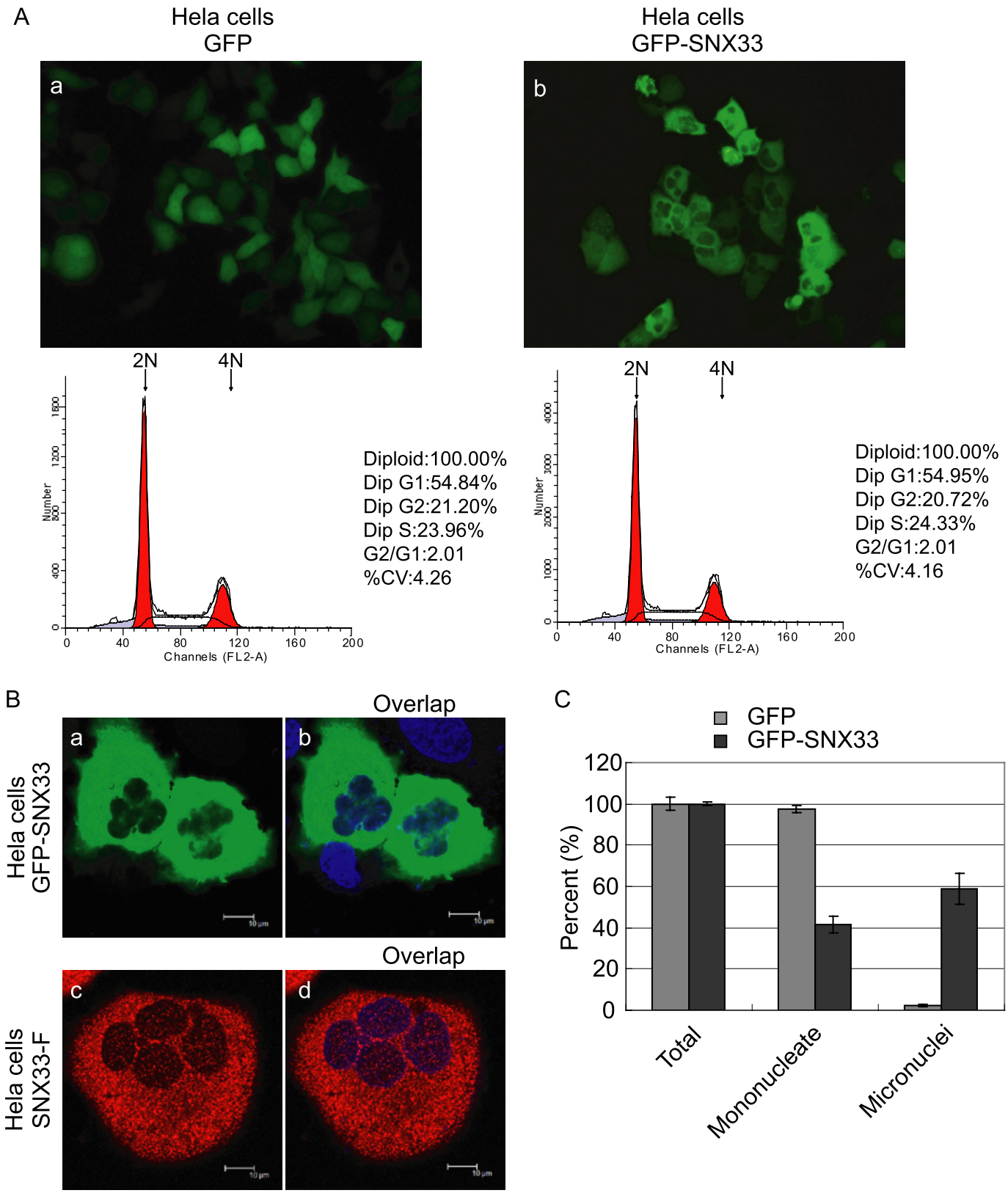

FIGURE 4. **Overexpression of SNX33 leads to micronucleated cells.** *A*, morphology and DNA content of HeLa cells transfected with GFP or GFP-SNX33. HeLa cells were transfected with GFP or GFP-tagged SNX33 and analyzed by confocal microscopy (*upper*) and FACS (*lower panel*) 24 h post-transfection as described under "Experimental Procedures." DNA contents (*2N* and *4N*) are indicated. *B*, micronucleated morphology of cells expressing SNX33. HeLa cells transfected with GFP- or FLAG- tagged SNX33 were fixed with 4% paraformaldehyde and then stained with 4′,6-diamidino-2-phenylindole or with anti-FLAG antibodies. Images were acquired by confocal microscopy. *C*, SNX33 induced almost 60% micronucleated phenotype. HeLa cells transfected with GFP or GFP-tagged SNX33 were photographed and then quantified to show the percentage of micronucleated cells.

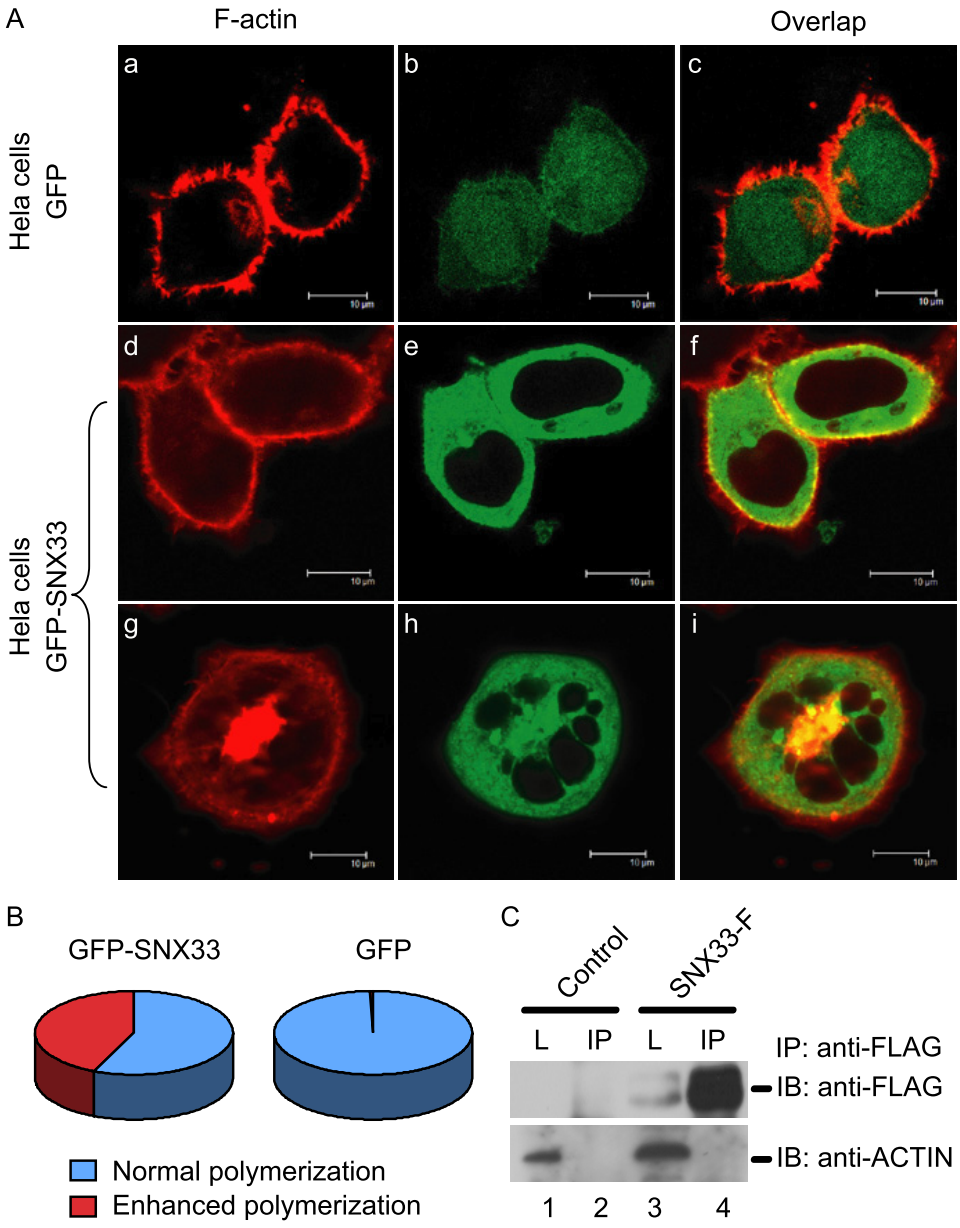

FIGURE 5. **SNX33 overexpression causes actin polymerization.** *A*, human SNX33 causes F-actin abnormal polymerization in cytoplasm. HeLa cells transfected with GFP or GFP-tagged SNX33 were fixed and stained with rhodamine-phalloidin. Note the micronucleated cells with F-actin polymerization clustered in the *middle of the cells* (*panels g*, *h*, and *i*). *B*, quantification of micronucleated cells in *A*. HeLa cells transfected as in *A* were processed and analyzed by confocal microscopy and quantified for micronucleated cells. *C*, SNX33 does not interact with actin. HEK293T cells transfected with the control vector or FLAG-tagged SNX33 were analyzed by co-immunoprecipitation (*IP*) assays using anti-FLAG resin for the pulldown and anti-ACTIN antibodies for the detecting interactions. *IB*, immunoblot. L, lysis.

purified SNX33 eliminated the signal completely (*c* and *e*). This antibody was then used to detect endogenous SNX33 proteins. We detected endogenous SNX33 expression in 13 human cell lines (A549, pro5, PC3, SPC-A1, NCI-H460, HT1080, Hlamp, HEK293T, LN4, GL82, L-78, MCF7, HeLa cells) with anti-SNX33 antibody (Fig. 1, *E* and *F*). We concluded that SNX33 protein is widely distributed in a variety of cell lines. We performed fluorescence immunostaining for the endogenous SNX33 in 4 human cell lines, including pro5, SPC-A1, HT1080, and Hlamp. As shown in Fig. 1*G*, the negative control did not detect any protein as predicted, and human SNX33 proteins are distributed in the cytoplasm of pro5, SPC-A1, HT1080 but not in Hlamp as expected. Taken together, human SNX33 does have an extensive expression profile.

SNX33 Knockdown Results in Abnormal Cell Morphology—To find out the function of SNX33 in cells, we knocked it down in different cell lines. GFP expression levels and Western blots (Fig. 2, *A* and *B*) showed that shRNA1, shRNA2 could significantly decrease the level of co-transfected SNX33 protein, and shRNA1 was more effective than shRNA2. We chose shRNA1 for further experiments. shRNA1 treatment also reduced the level of endogenous SNX33 in MCF7 and HeLa cells (Fig. 2*C*). We found that knockdown of SNX33 caused huge morphological changes in these cells. They appeared as neural-like cells with multi-tentacles (Fig. 2*D*). These morphological changes were further demonstrated in WASp, γ-tubulin, and F-actin staining (Fig. 2*E*). We failed to detect expression changes of several neural cell markers by Western blot and immunostaining (data not shown). We tried but failed to establish stable cell lines constitutively expressing SNX33 shRNA in HeLa or MCF7 cells. So we selected the transfected cells by hygromycin for 7 days and used FACS to examine whether there was any change in cell cycle or apoptosis. Fig. 2*F* indicated the G_1 phase of the transfected cell was delayed and the S phase was shortened. The annexin V apoptosis detection assay showed that the percentage of the apoptotic cells in transfected HeLa and MCF7 cells was significantly raised (Fig. 2*G*). These results suggest that inhibition of endogenous SNX33 induces cell cycle arrest, which may induce abnormal cell morphology and enhanced apoptosis rate.

SNX33 Overexpression Blocks Cell Division in HeLa Cells—In the case of SNX33 playing functions in cell cycle and cell skeleton, what about the situation of SNX33 overexpression. To probe its function, we constructed an expression vector for GFP-SNX33 fusion protein (Fig. 3*A*), and this construct expressed the correct protein in transfected cells (Fig. 3*B*). We then tried to generate stable cell lines that would express this GFP-SNX33 constitutively. To our surprise, we failed repeatedly to establish such cell lines. To figure out why cells expressing SNX33 failed to form colonies, we performed lineage anal-

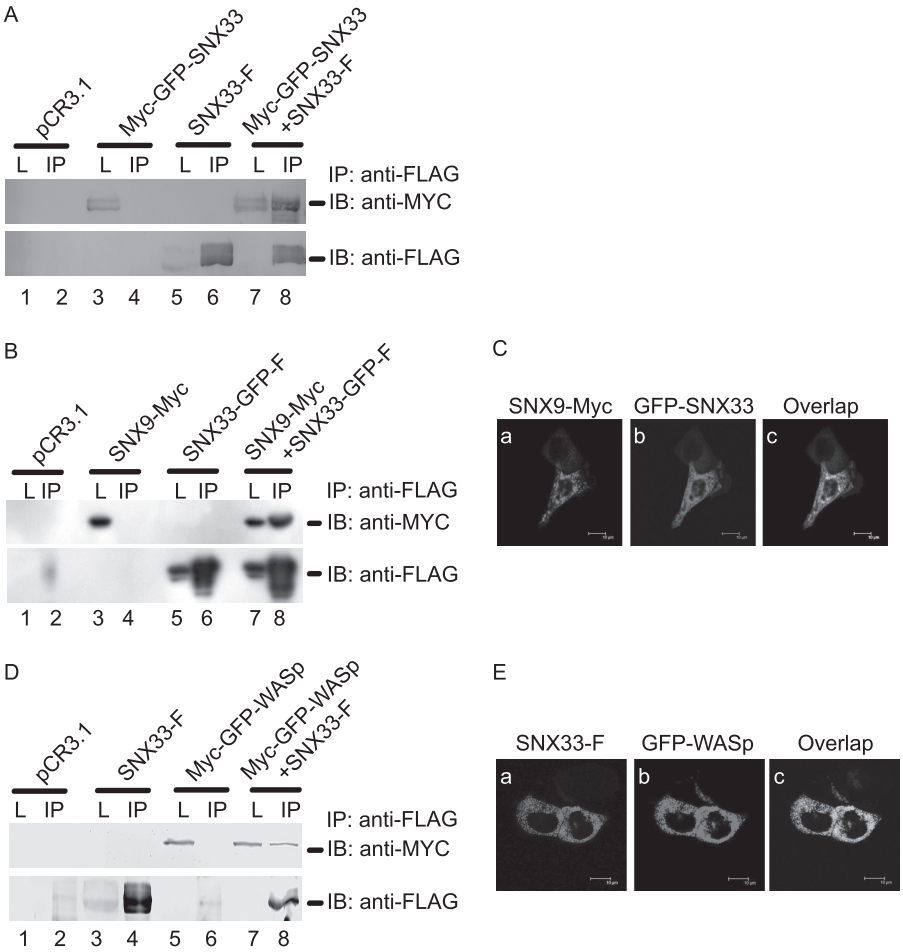

FIGURE 6. **SNX33 interacts with itself, SNX9, and WASp.** *A*, homotypic interaction of SNX33. pCR3.1 vector (4 μg, *lane 1*-2), SNX33 fusion with Myc and GFP tag (4 μg), or SNX33 fusion with a FLAG tag (4 μg) was either transfected alone (*lanes 3* and *4* or *5* and *6*) or together (*lanes 7–8*) into HEK293T cells. Cell lysates were analyzed for protein expression (*lanes 1*, *3*, *5*, and *7*) or for interactions by immunoprecipitation (*IP*) followed by Western blotting (*IB*) as described under "Experimental Procedures" (*lanes 2*, *4*, *6*, and *9*). Human SNX33 interacts with itself. L, lysis. *B*, SNX33 interacts with SNX9. The transfections and analyses were carried out as in *A*. *C*, co-localization of SNX33 and SNX9. HeLa cells transfected with SNX9-Myc and GFP- and FLAG-tagged SNX33 (*GFP-SNX33*) were stained with anti-MYC antibodies and detected with TRITC-conjugated goat anti-rabbit antibodies and then scanned by Leica confocal systems as described under "Experimental Procedures." *D*, SNX33 interacts with WASp. The transfections and analyses were carried out as in *A*. *E*, co-localization of SNX33 and WASp. The transfections and stainings were executed as in *C*.

ysis for cells transfected with GFP or GFP-SNX33 as shown in Fig. 3, *C* and *D*. Although HeLa cells with GFP could form a lot of colonies that we could see (*a*, *c*, and *e*), cells with GFP-SNX33 failed to divide (*b*, *d*, and *f*), thus, providing an explanation for the failed attempts to generate SNX33 stable lines. To localize the protein sequence responsible for this inhibitory activity, we analyzed the six deletion mutants of SNX33 with adequate expression (Fig. 3, *A* and *B*). Except GFP-D1 (only with SH3 domain), the rest of the mutants remain inhibitory to cell proliferation (Fig. 3, *E* and *F*). These results demonstrate that overexpression of human SNX33 disrupts the normal cell division.

SNX33 Expression Induces Micronucleation—Upon careful examination, we uncovered that SNX33 triggers cells to undergo micronucleation (Fig. 4*A*, *panel b versus a*). Compared with GFP-transfected cells, cells expressing GFP-SNX33 contain multiple small nuclei (Fig. 4*A*) yet without alteration in the DNA contents. The percentage of these micronuclei-like cells was nearly 60% in GFP-SNX33 cells (Fig. 4, *A* and *C*) but non-existent in GFP-transfected cells. Further analysis by confocal microscopy revealed that the nuclei of GFP-SNX33-transfected cells have been cleaved into multiple micronuclei (Fig. 4*B*).

SNX33 Expression Causes F-actin Abnormal Polymerization—Evidence presented so far suggests that SNX33 may impact cytokinesis through actin polymerization. To test this possibility, we stained for F-actin, which reflected specific filamentous actin localization. As shown in Fig. 5*A*, actin filaments in HeLa cells transfected with GFP are mostly distributed at the cell peripheral area (*a*, *b*, and *c*). However, actin filaments in SNX33-transfected HeLa cells are distributed in two main categories; (i) cells with normal nuclei have normal actin distribution (*d*, *e*, and *f*), and (ii) cells with micronuclei have polymerized actin bundles localized at the center with enriched localization of SNX33 as well (*g*, *h*, and *i*). Compared with cells with GFP, the percentage of enhanced actin polymerization is nearly 60% in cells with SNX33 (Fig. 5*B*). However, when we tested if SNX33 and actin interact with each other, the result is negative (Fig. 5*C*). We concluded that SNX33 enhanced F-actin polymerization indirectly.

SNX33 Interacts with Itself, SNX9, and Also with WASp—Many SNXs have been shown previously to form homodimers such as demonstrated for SNX9 (14). To test this possibility for SNX33, we co-transfected FLAG-tagged SNX33 with Myc- and GFP-tagged SNX33 into HEK293T cells and performed a co-immunoprecipitation assay using anti-FLAG resin and detected with anti-Myc antibody as described under "Experimental Procedures." As shown in Fig. 6*A*, Myc- and GFP-tagged SNX33 (*lane 8*, *upper band*) was co-precipitated with FLAG-tagged SNX33 (*lane 8*, *lower band*), confirming that SNX33 could form homodimers. As members of the SNX family tend to form heterodimers (3–5, 7), we tested if SNX33 interacts with one of its close relatives (11). As shown in Fig. 6*B*, Myc-tagged SNX9 (*lane 8*, *upper band*) was co-precipitated with GFP- and FLAG-tagged SNX33 (*lane 8*, *lower band*), confirming that human SNX33 did have the ability to form heterodimers with another SNX. We further confirmed that SNX33 and SNX9 also co-localize intracellularly (Fig. 6*C*).

Because SNX9 interacts with WASp, we hypothesize that SNX33 may also interact with WASp (15, 21). To test this

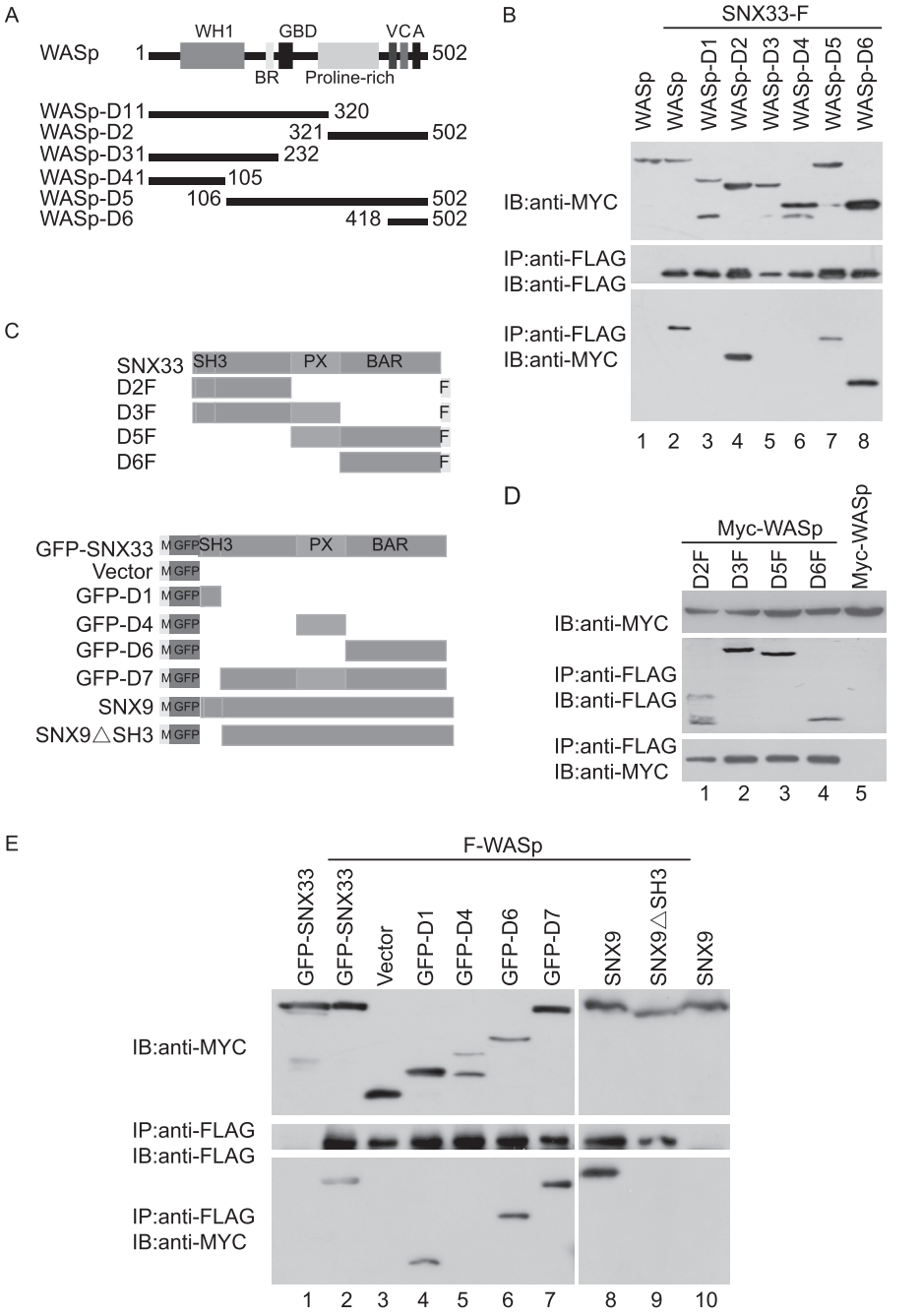

FIGURE 7. **SNX33 interacts with VCA domain of WASp through multi-domains.** *A*, the scheme depicts the respective domain contained in WASp and its deletions (*WASp-D1–6*). *WH1*, WASp homology domain 1; *BR*, basic region; *GBD*, GTPase binding domain; *Proline-rich*, praline-rich domain; *VCA*, verprolin, central, acidic domains, which interacts with ARP2/3 complex. *B*, SNX33 interacts with WASp through the VCA domain. Deletion mutants of WASp with the Myc tag and SNX33-F were co-expressed in HEK293T cells, immunoprecipitated (*IP*) with anti-FLAG resin, and detected as indicated. *IB*, immunoblot. *C*, the scheme depicts the respective domain contained in SNX33 (GFP-SNX33), SNX33 deletions (D2F, D3F, D5F, D6F and GFP-D1, GFP-D4, GFP-D6, GFP-D7), SNX9, and SNX9ΔSH3. *SH3*, Src homology 3 domain; *PX*, phox homology domain; *BAR*, Bin/Amphiphysin/Rvs domain. *D*, co-immunoprecipitation of Myc-tagged WASp with FLAG-tagged SNX33 deletions with indicated antibodies. *E*, co-immunoprecipitation of FLAG-tagged WASp with Myc and GFP-tagged SNX33 deletions, control vector, SNX9, and SNX9ΔSH3 with indicated antibodies.

hypothesis, we cloned WASp to a mammalian expression vector and designed a co-immunoprecipitation assay. As shown in Fig. 6*D*, GFP- and Myc-tagged WASp was precipitated with FLAG-tagged SNX33 (*lane 8*). As shown in Fig. 6*E*, GFP-tagged WASp diffused with a punctate pattern as expected and colocalized with SNX33. These results demonstrate that SNX33 interacts and colocalizes with SNX9 and WASp.

SH3 and BAR Domains of SNX33 Interact with the VCA Domain of WASp Directly—To map the domains in WASp and SNX33 required for their interaction, we designed six deletions of WASp (WASp-D1, WASp-D2, WASp-D3, WASp-D4, WASp-D5, WASp-D6) and eight deletions of SNX33 (D2F, D3F, D5F, D6F, GFP-D1, GFP-D4, GFP-D6, and GFP-D7) (Fig. 7, *A* and *C*). Full-length SNX33 was precipitated with full-length WASp, WASp-D2, WASp-D5, and WASp-D6 but not WASp-D1, WASP-D3, and WASp-D4 (Fig. 7*B*). Therefore, we conclude that the VCA domain, which is responsible for ARP2/3 complex binding (28, 29), is also required for WASp to interact with SNX33. On the other hand, all the SNX33 deletions (D2F, D3F, D5F, and D6F) appear to co-precipitate with WASp (Fig. 7*D*). The interaction between SNX33 and WASp was maintained in GFP-D1 (SH3 domain), GFP-D6 (BAR domain), and GFP-D7 but not GFP-D4. These data reveal that either the SH3 or the BAR domain in SNX33 is sufficient for WASp binding. This is in contrast to SNX9 in which the SH3 domain is essential for its interaction with WASp (Fig. 7*E* and Ref. 15). Taken together, we conclude that SNX33 can interact with the VCA domain of WASp through either the SH3 or the BAR domain.

WASp Phenocopies SNX33 When Ectopically Expressed in HeLa Cells, and the Knockdown of WASp Alleviates the Phenotype Induced by SNX33—The direct interaction between SNX33 and WASp suggests that SNX33 may mediate its function through WASp. To test this hypothesis, we transfected GFP-tagged WASp into HeLa cells. Compared with GFP vector control, we found that HeLa cells with high WASp expression could not divide, similar to those cells expressing SNX33 (Fig. 8*A*). The growth curve confirmed the same conclusion that WASp blocked cell division (Fig. 8*B*), thus phenocopying SNX33. Furthermore, we also found that the micronucleated phenotype induced by SNX33 was inhibited by about 50% when endogenous WASp was knocked down with

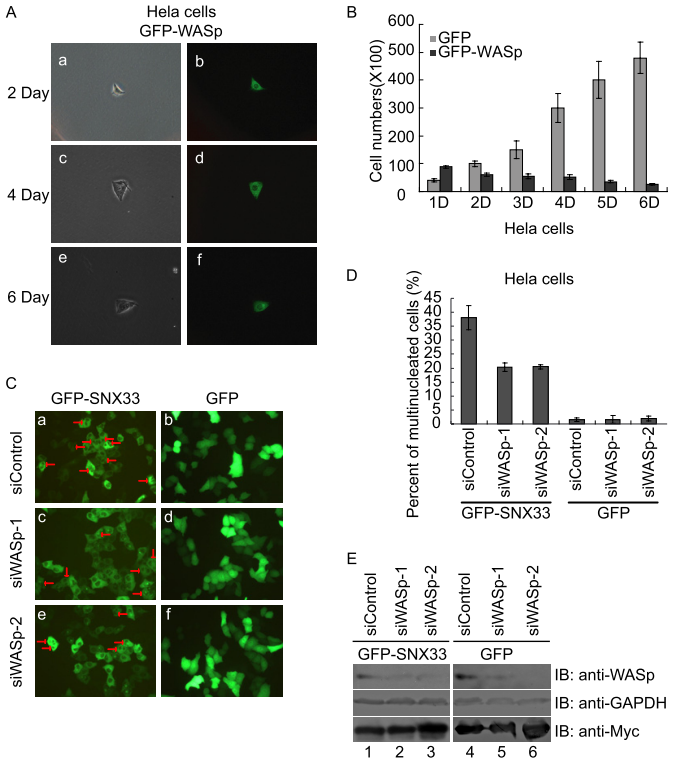

FIGURE 8. **WASp phenocopies SNX33 when ectopically expressed in HeLa.** *A*, ectopic expression of WASp blocks cell division as SNX33. HeLa cells transfected with GFP-tagged WASp were cultured, selected, and then photographed for 6 days to show its inhibitory effect on HeLa cell division. *B*, growth curve of GFP- or WASp-transfected HeLa cells. HeLa cells transfected with GFP or GFP-tagged WASp (*GFP-WASp*) were split into a 96-well plate with 5 wells each, cultured, and then counted daily. *C*, the effect of WASp siRNA on the micronucleated phenotype of SNX33. HeLa cells transfected with GFP-tagged SNX33 or GFP and siControl, siWASp-1, siWASp-2 were captured by Olympus digital cameral. Note: *red arrows* indicate the micronucleated cells. *D*, siRNAs of WASp reduce the micronucleated phenotype by 50%. HeLa cells transfected with GFP-tagged SNX33 or GFP and siControl, siWASp-1, siWASp-2 were photographed and then quantified to show the percentage of micronucleated cells. *E*, efficient knockdown of endogenous WASp in HeLa cells. HeLa cells transfected with Myc-tagged GFP or Myc- and GFP-tagged SNX33 together with siControl, siWASp-1, or siWASp-2 were analyzed as described under "Experimental Procedures." Note the effective reduction of WASp in siWASp-1- or siWASp-2-treated cells (*panels 2* and *5* or *3* and *6*). *IB*, immunoblot. *GAPDH*, glyceraldehyde-3-phosphate dehydrogenase.

specific siRNAs (Fig. 8, *C* and *D*). Consistently, the endogenous WASp was inhibited effectively by both siRNAs as shown in Fig. 8*E*. These results strongly suggest that SNX33 functions through WASp in regulating cytokinesis.

DISCUSSION

In this report we identified SNX33 as a novel member of the SNX family. SNX33 is widely expressed in many tumor cells or cell lines. Knockdown of this gene results in the morphology, cell cycle progression, and apoptosis rate changes in HeLa and MCF7 cells. These changes may come from the actin dysfunction. We also found that SNX33 and WASp, when ectopically expressed, were able to halt cytokinesis in HeLa cells or MCF7 cells. This function has never been reported previously and may help explain many cellular activities in cell division and cytoskeleton. We were surprised that cells are so sensitive to activities associated with SNX33 and WASp expression initially. We then found that SNX33 interacts with the VCA

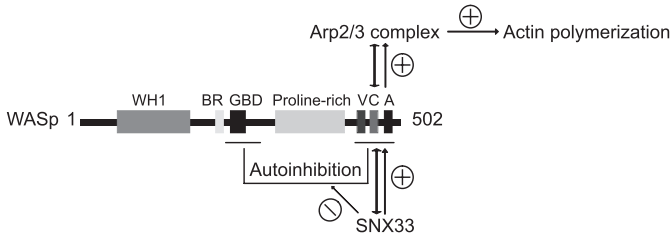

FIGURE 9. **A proposed model of SNX33 function.** We present a model that SNX33 interacts with WASp via the VCA autoinhibition domain to activate WASp, which presumably promotes Arp2/3 complex formation and actin polymerization. Prolonged actin polymerization disables cell division and fragments the nucleus into multiple sub-nuclei. In shRNA experiments, SNX33 is depleted, which may impair actin polymerization during normal cell cycle, leading to distorted cell shape and morphology. *WH1*, WASp homology domain 1; *BR*, basic region; *GBD*, GTPase binding domain; *Proline-rich*, praline-rich domain; *VCA*, verprolin, central, acidic domains.

domain of WASp, which has been known to autoinhibit WASp by interacting with the GTPase binding domain (30). The binding of SNX33 to the VCA domain could relieve the autoinhibition, leading to an increase of WASp activity (Fig. 9). As WASp can induce ectopic actin polymerization (31) and cause abnormal cytokinesis (22), we propose that SNX33 functions through WASp. This was supported by the facts that WASp phenocopies SNX33 when expressed in HeLa under similar conditions, and the knockdown of endogenous WASp alleviated the micronucleated phenotype triggered by SNX33 (Fig. 8). Finally, given the effect observed for SNX33 overexpression or knockdown in HeLa or MCF7 tumor cells, SNX33 could be a potential target for anti-cancer drug development.

Acknowledgments—We thank Dr. I. Chambers for the pPyCAGIP plasmid, Dr. Stefan F. Lichtenthaler for control, shRNA1, and shRNA2 plasmids. We also thank Dr. X. Shu for beneficial revision. We thank Y. Q. Ding, B. M. Qin, L. Y. Huang, K. S. Chen, and other members of the Pei laboratory for assistance and general encouragement.

REFERENCES

1. Kurten, R. C., Cadena, D. L., and Gill, G. N. (1996) *Science* **272,** 1008–1010
2. Ponting, C. P. (1996) *Protein Sci.* **5,** 2353–2357
3. Haft, C. R., de la Luz Sierra, M., Bafford, R., Lesniak, M. A., Barr, V. A., and Taylor, S. I. (2000) *Mol. Biol. Cell* **11,** 4105–4116
4. Kurten, R. C., Eddington, A. D., Chowdhury, P., Smith, R. D., Davidson, A. D., and Shank, B. B. (2001) *J. Cell Sci.* **114,** 1743–1756
5. Worby, C. A., and Dixon, J. E. (2002) *Nat. Rev.* **3,** 919–931
6. Otsuki, M., Itoh, T., and Takenawa, T. (2003) *J. Biol. Chem.* **278,** 6461–6469
7. Parks, W. T., Frank, D. B., Huff, C., Renfrew Haft, C., Martin, J., Meng, X., de Caestecker, M. P., McNally, J. G., Reddi, A., Taylor, S. I., Roberts, A. B., Wang, T., and Lechleider, R. J. (2001) *J. Biol. Chem.* **276,** 19332–19339
8. Howard, L., Nelson, K. K., Maciewicz, R. A., and Blobel, C. P. (1999) *J. Biol. Chem.* **274,** 31693–31699
9. Lin, Q., Lo, C. G., Cerione, R. A., and Yang, W. (2002) *J. Biol. Chem.* **277,** 10134–10138
10. Qin, B., He, M., Chen, X., and Pei, D. (2006) *J. Biol. Chem.* **281,** 36891–36896
11. Seet, L. F., and Hong, W. (2006) *Biochim. Biophys. Acta* **1761,** 878–896
12. Schöbel, S., Neumann, S., Hertweck, M., Dislich, B., Kuhn, P. H., Kremmer, E., Seed, B., Baumeister, R., Haass, C., and Lichtenthaler, S. F. (2008) *J. Biol. Chem.* **283,** 14257–14268
13. Heiseke, A., Schöbel, S., Lichtenthaler, S. F., Vorberg, I., Groschup, M. H., Kretzschmar, H., Schätzl, H. M., and Nunziante, M. (2008) *Traffic* **9,**

1116–1129
14. Childress, C., Lin, Q., and Yang, W. (2006) *Biochem. J.* **394,** 693–698
15. Badour, K., McGavin, M. K., Zhang, J., Freeman, S., Vieira, C., Filipp, D., Julius, M., Mills, G. B., and Siminovitch, K. A. (2007) *Proc. Natl. Acad. Sci. U.S.A.* **104,** 1593–1598
16. Yarar, D., Surka, M. C., Leonard, M. C., and Schmid, S. L. (2008) *Traffic* **9,** 133–146
17. MaCaulay, S. L., Stoichevska, V., Grusovin, J., Gough, K. H., Castelli, L. A., and Ward, C. W. (2003) *Biochem. J.* **376,** 123–134
18. Thrasher, A. J. (2002) *Nat. Rev. Immunol.* **2,** 635–646
19. Marchand, J. B., Kaiser, D. A., Pollard, T. D., and Higgs, H. N. (2001) *Nat. Cell Biol.* **3,** 76–82
20. Machesky, L. M., and Insall, R. H. (1998) *Curr. Biol.* **8,** 1347–1356
21. Cory, G. O., Cramer, R., Blanchoin, L., and Ridley, A. J. (2003) *Mol. Cell* **11,** 1229–1239
22. Moulding, D. A., Blundell, M. P., Spiller, D. G., White, M. R., Cory, G. O., Calle, Y., Kempski, H., Sinclair, J., Ancliff, P. J., Kinnon, C., Jones, G. E., and Thrasher, A. J. (2007) *J. Exp. Med.* **204,** 2213–2224
23. Pan, G., Qin, B., Liu, N., Schöler, H. R., and Pei, D. (2004) *J. Biol. Chem.* **279,** 37013–37020
24. Jiang, A., and Pei, D. (2003) *J. Biol. Chem.* **278,** 38765–38771
25. Tsuboi, S., Nonoyama, S., and Ochs, H. D. (2006) *EMBO Rep.* **7,** 506–511
26. Olivier, A., Jeanson-Leh, L., Bouma, G., Compagno, D., Blondeau, J., Seye, K., Charrier, S., Burns, S., Thrasher, A. J., Danos, O., Vainchenker, W., and Galy, A. (2006) *Mol. Ther.* **13,** 729–737
27. Tsuboi, S., and Meerloo, J. (2007) *J. Biol. Chem.* **282,** 34194–34203
28. Rohatgi, R., Ma, L., Miki, H., Lopez, M., Kirchhausen, T., Takenawa, T., and Kirschner, M. W. (1999) *Cell* **97,** 221–231
29. Machesky, L. M., Mullins, R. D., Higgs, H. N., Kaiser, D. A., Blanchoin, L., May, R. C., Hall, M. E., and Pollard, T. D. (1999) *Proc. Natl. Acad. Sci. U.S.A.* **96,** 3739–3744
30. Kim, A. S., Kakalis, L. T., Abdul-Manan, N., Liu, G. A., and Rosen, M. K. (2000) *Nature* **404,** 151–158
31. Symons, M., Derry, J. M., Karlak, B., Jiang, S., Lemahieu, V., Mccormick, F., Francke, U., and Abo, A. (1996) *Cell* **84,** 723–734